



Cutting edge preparation of micro end mills by PVD-etching technology

Christoph Paul Jäckel¹ · Alexander Leonard Meijer¹ · Dominic Stangier^{2,3} · Nelson Filipe Lopes Dias² · Wolfgang Tillmann² · Dirk Biermann¹

Received: 22 September 2023 / Accepted: 11 December 2023 / Published online: 15 February 2024
© The Author(s) 2024

Abstract

Micromilling tools face significant challenges in achieving cutting edge preparation by mechanical processes due to their small size. To address these limitations, a new approach for cutting edge preparation of micro end mills by physical vapor deposition (PVD) etching technology is presented. By adapting the etching strategy, which is conventionally used as pre-treatment process for PVD technology to clean and condition the surface of cemented carbide substrate, cutting edges of micromilling tools were successfully modified. The high-energy process variation by Advanced Arc-Enhanced Glow Discharge (AEGD) offers the possibility of achieving high material removal rates on the tool surfaces and thereby altering the cutting edge geometry. Fundamental investigations on material removal as well as on the effects on surface topography, sub-surface properties, and coating adhesion of a subsequently applied PVD coating are performed. To influence the topography and the cutting edge geometry, the preparation time t_p and bias voltage U_B were selected. Subsequently, the machining performance of the modified tools is evaluated in a micromilling process of the hardened powder-metallurgical high-speed steel AISI M3:2 with a hardness of 62 ± 1 HRC. For this purpose, micro end mills of cemented carbide with a diameter of $D = 1$ mm were conditioned, achieving asymmetric geometric properties of cutting edges with varying average cutting edges rounding of $\bar{S} = 5.8 \dots 14.8 \mu\text{m}$ and a form-factor of $K = 2.0 \dots 2.7$. Based on the application tests a positive influence on the process forces was found. Thus, an efficient approach to cutting edge preparation can be identified by specifically designing ion etching in the PVD coating process.

Keywords Micromilling · Physical vapor deposition · Cutting edge preparation · Asymmetrical cutting edge geometry · Advanced Arc-Enhanced Glow Discharge

1 Introduction

The performance and wear behavior of cutting tools depends not only on the cutting material and the use of wear resistant coatings but also on the condition of the cutting edge. Due to this, preparations of cutting edges have been widely established and were the subject of various investigations [1, 2]. Fine machining of the cutting edge reduces defects

such as microscopic breakouts or burrs achieving a defined shape, improving thereby the cutting performance due to an enhanced cutting edge stability [3, 4]. Depending on the application, different cutting edge designs featuring a rounding, chamfers, or combinations of both have been established [5, 6]. Characterizations of rounded cutting edge geometries are mainly based on the characteristic values of the cutting edge radius r_β and the parameters of the form-factor method according to *Denkena* [7]. In general, the preparation of the cutting edges enhances the wear resistance by reducing chipping and initial cracking formation of the substrate as well as increasing its mechanical stability due to the changed geometry [8]. On the other hand, however, based on experimental results, it can be stated that an increasing size of the cutting edge geometry, e.g. rounding, results in rising cutting forces as well as feed forces [9, 10]. Furthermore, a sufficient design of the preparation process improves the

✉ Christoph Paul Jäckel
christoph.jaekel@tu-dortmund.de

¹ Institute of Machining Technology, TU Dortmund University, Baroper Straße 303, 44227 Dortmund, Germany

² Institute of Materials Engineering, TU Dortmund University, Leonhard-Euler-Str. 2, 44227 Dortmund, Germany

³ Oerlikon Balzers Coating Germany GmbH, Am Böttcherberg 30-38, 51427 Bergisch Gladbach, Germany

adhesion of applied wear protection coatings [11]. *Denkena* et al. showed for the machining of AISI 1045 that the process forces are mainly affected by the cutting edge segment of the flank face S_α [12]. Similar results by *Bassett* et al. support the unfavorable influence of the flank face sided rounding of the cutting edge on the cutting forces [1]. Comparable effects were observed by *Fang* and *Wu* machining aluminum alloys with bevel-like cutting edge shapes [13]. According to *Shaw* this can be attributed to effects in the chip formation process, e.g. extended shear zone with sub-surface plastic material flow, depending on the microgeometry of the cutting edge geometry [14]. A larger cutting edge segment on the flank face S_α therefore results in a stronger plastic deformation and ploughing of the workpiece material. This has also been observed in the case of chamfered cutting edge geometries [10, 15]. Thus a more beneficial impact on the cutting process can be achieved with an asymmetric cutting edge geometry with a form-factor $K > 1$ by focusing the preparation on the rake face. Furthermore, the potential of the modification in general depends on the adaptation of the cutting edge geometry to the respective cutting process as well as the application scenario, e.g. workpiece material and tool geometry [1, 9, 12]. In order to achieve this, a variety of different preparation methods such as abrasive jet machining, brushing, and drag finishing are used in the field of conventional macromachining processes, which have already been extensively investigated [1, 16, 17].

Besides conventional machining, micromachining offers promising potential for the field of die and mold manufacturing. In addition to high achievable shape and dimensional accuracy and surface quality in combination with a favorable impact on the sub-surface zone of the workpiece micromachining offers possibility to enhance the operational behavior and increase the fatigue behavior of filigree and yet highly stressed components and molds [18–20]. Particularly in the field of hard machining, the small cutting tools achieve only short tool lives, which limits the resource-efficient application of these processes [21]. For this reason, current efforts are focused on utilizing the potential of cutting edge preparation in order to enhance the tool life in micromachining. *Uhlmann* et al. demonstrated the possibility of a cutting edge preparation of filigree tools with a diameter of $D = 1$ mm using drag finishing [22]. Furthermore, they showed possibilities of polish blasting, brush polishing, and magnet finishing on tools with $D = 0.5$ mm [23]. *Krebs* et al. modified end mills ($D = 1$ mm) by pressurized wet abrasive jet machining and showed basic potentials of cutting edge preparation for improving coating adhesion at the cutting edge [24]. The preparation methods considered so far allow the adjustment of varying cutting edge rounding. Furthermore, potentials for improving the application behavior and

wear resistance of micro end mills have already been demonstrated [23]. However, even taking into account further investigations, the setting of asymmetric cutting edge shapes has so far been a major challenge. In particular for establishing small cutting edge geometries, which are appropriate considering the process of micromachining, mechanical preparation methods are severely limited and only allow the defined setting of an asymmetrical shape to a very limited extent.

In addition to mechanical pre-treatments a removal of material at the cutting edge can also be achieved by plasma-based etching processes. Usually, ion etching (IE) is used to clean and condition the substrate surface prior to the deposition of the coatings in order to improve the adhesion of coatings to the substrate [25]. As an in situ cleaning process, it can be carried out in the coating device and has become an established process due to the possibility to remove contaminations located on the surface [26]. The generation of the plasma respectively the free ions is usually based on a glow discharge, which is triggered by an electrical potential in the deposition chamber. The free ions are then accelerated to the substrate by an electrical potential, which is applied by a bias voltage U_B to the substrate holder system respectively the cutting tools. This results in an ion bombardment of the surface, which removes oxides and contaminations located at the surface. The bombardment with high-energy ions causes a momentum transfer on the surface atoms, which results in sputtering of the substrate surface. This alters the topography surface as well as microstructure and morphology of the sub-surface. Impacts of high-energy ions can also cause the formation of defects or implantation of ions in the sub-surface zone [27, 28]. In the case of etching cemented carbide, an increased removal of the cobalt (Co) binder phase can be observed, which leads to exposure of the tungsten carbides and thus to increased surface roughness [29]. Ion etching is carried out using both metallic and non-metallic ions [30, 31]. Ion etching with argon ions (Ar^+) is widespread due to the inert character avoiding interactions and chemical reactions with the substrate surface. Ar^+ etching with high bias voltages and consequently high kinetic energy can lead to the formation of surface regions providing additional nucleation sites for coating growth. Due to the randomly orientated grain nucleates, competitive growth and formation of fibrous columns separated by open grain boundaries result. This affects the hardness of the coating and thus results in a deterioration of the wear behavior of the tools [25, 31]. Regular Ar^+ ion etching processes only achieve low removal rates, hence such process steps are only used for surface conditioning. However, *Gassner* et al. mentioned in their investigations an influence of Ar^+ ion etching on the microgeometry of cutting inserts [29]. To further increase the ionization

in the working chamber an arc-enhanced glow discharge (AEGD) process offers a promising approach for a highly efficient etching technology [32, 33]. By igniting a shielded arc evaporation (Arc) on a titanium cathode, a high amount of free electrons are generated and directed into the coating chamber by anodes. The generated electrons cause the ionization of argon atoms and thus to significantly increased proportions of Ar^+ ions in the plasma close to the handling system. This technological approach makes it possible to form plasmas with higher ion density and thus also significantly increased etch rates. Furthermore, AEGD-IE offers the possibility to utilize the effects shown by *Gassner* et al. in order to achieve a targeted modification of the microgeometry of cutting edges.

This article presents fundamental investigations on substrates of ultrafine grain cemented carbide in order to describe the etch rate and the influence on the constitution of the surface and sub-surface properties. Subsequently, the alteration of the cutting edge shape of uncoated micro end mills is presented. As will be shown, it is possible to create varying cutting edge geometries. Additionally, the preparation approach made it possible to reliably produce oriented cutting edges with a form-factor of $K > 1$. In order to evaluate the cutting performance, tools were modified and coated with a TiAlSiN coating deposited by High Power Impulse Magnetron Sputtering (HiPIMS). The evaluation of the operational and wear performance was conducted in a micromilling process of the hardened HSS AISI M3:2 with a hardness of 62 ± 1 HRC showing reduced wear and improved process performance.

2 Materials and methods

2.1 Materials

2.1.1 Substrate material for complementary analysis

The Advanced AEGD-IE and coating experiments were carried out on ultrafine grain carbide of type HB20UF (Boehlerit, Austria) with WC/Co 8 wt.% and a grain size of $d_k = 0.2 \dots 0.5 \mu\text{m}$. The coin-shaped substrates with a diameter of $D = 20$ mm and a height of $h = 5$ mm were selected according to conventional, uncoated micro end mills for comparability. The substrates exhibited a fine ground topography in the initial state with an arithmetic mean roughness of $R_a = 3.2 \pm 0.2$ nm and a maximum height of roughness profile of $R_z = 20.5 \pm 0.8$ nm. In addition, the analysis by x-ray diffraction revealed isotropic compressive residual

Table 1 Chemical composition of AISI M3:2 (wt.%)

C	Cr	Mo	V	W	Fe
1.28	4.00	5.00	3.10	6.40	Balanced

stresses in the WC-phase of $\sigma_{\text{avg}} = 223.2 \pm 15.5$ MPa of the initial surface.

2.1.2 Workpiece material

For this study, the operational and wear behavior of the tools were examined in the machining of AISI M3:2 high-speed steel. Due to its powder metallurgical production, a homogeneous distribution of carbides with a size between 2 and $6 \mu\text{m}$ is achieved. The chemical composition of the material is presented in Table 1. All investigated specimens were vacuum hardened and tempered three times to a hardness of approx. 62 ± 1 HRC. Due to its mechanical properties, including a tensile strength of over 2000 N/mm, this material is particularly suitable for die and mold manufacturing in the application field of metal forming processes. However, these properties lead to a high thermo-mechanical load on the tools used in the micromilling process, resulting in a short tool life. An optimization of the micromilling tools by cutting edge preparation thus represents a promising approach.

2.1.3 Micro end mills

The preparation of the cutting edges and the machining experiments were carried out with two fluted micro end mills with a diameter of $D = 1$ mm and a corner radius of $r_e = 50 \mu\text{m}$. The tools are based on the Peakcook Series 599 by Zecha Hartmetall-Werkzeugfabrikation GmbH, but featured a shortened neck length of $l_2 = 0.5$ mm and were provided in uncoated condition. In the initial state, the tools already exhibited a uniform cutting edge with an average edge rounding of $\bar{S} = 3.5 \pm 0.3 \mu\text{m}$. The tools as well as the initial state of the cutting edge can be seen in Fig. 1.

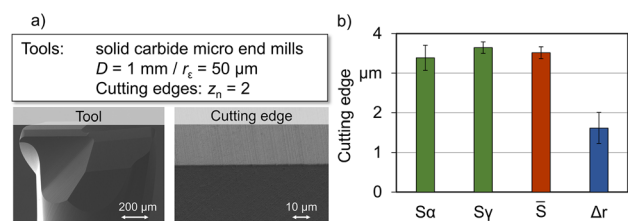


Fig. 1 a Micro end mill and b the initial condition of the cutting edge

2.2 PVD technology

The variation of the etching process and deposition of the PVD coatings were performed on a customized METAPLAS.DOMINO kila flex (Oerlikon Balzers Coating Germany GmbH, Germany) coater. The device offers the opportunity to perform deposition processes by cathodic arc evaporation as well as sputtering technology using different types of power supplies, such as HiPIMS. Prior to the deposition process, the substrates and tools were cleaned by an ultrasonic bath with isopropanol for 15 min. The coin-shaped samples were mounted on the handling system using two-fold rotation, whereas the tools were placed in cups using three rotation axes.

The chamber was evacuated to a base pressure below $p < 4 \times 10^{-5}$ mbar and heated two times for one hour to degase the deposition chamber and heat the substrates. Subsequently, the etching process of the cemented carbide substrates was performed according to the design of experiments (Sect. 2.5) using the Advanced AEGD technology. As electron source, a shielded Ti-cathode operating at a current of $I_{\text{AEGD}} = 150$ A with four independently controlled anodes over the coating height was used to enable a flexible and variable etching process. The oxygen level inside the chamber is reduced by the evaporated Ti acting as a getter material. The ionized Ar atoms are attracted by the bipolar asymmetric pulsed bias potential with a frequency of $f = 20$ kHz using different levels of bias voltages and etching times.

Subsequently, the PVD coating process was carried out for the coin-shaped substrates by using cathodic arc evaporation technology with controllable coil systems for the magnetic fields on the evaporators. The deposited TiAlN coating had a coating thickness of approximately $t = 2.0$ μm with a hardness of $H = 39.3 \pm 3.4$ GPa and a Young's modulus of $E = 534.9 \pm 44.5$ GPa. For the application tests of the micro end mills, magnetron sputtering technology was used running in HiPIMS mode. The applied HiPIMS-TiAlSiN coating had a hardness of $H = 29.6 \pm 2.1$ GPa and a Young's modulus of $E = 325.7 \pm 25.3$ GPa. The deposition time was adjusted to grow HiPIMS-TiAlSiN with a thickness of 2.5 μm .

2.3 Analytical Methods

2.3.1 Analysis of the material removal and etch rate

The adaptation of the Advanced AEGD-IE for a cutting edge conditioning was initially investigated in analogy tests on coin-shaped substrates of cemented carbide. By locally masking each sample with a titanium oxide coat prior to the experiments the etch rate as well as the changes in the topography could be analyzed. After processing the masking was removed. This allowed the determination of the step height

between the initial and the etched surface and thus the etch rate by consideration of the process time.

2.3.2 Surface analysis

Surface topographies were examined with the 3D optical measuring microscope DuoVario (Confovis GmbH, Germany), which was equipped with a MAG-50x-lens (Olympus, Japan) with a numerical aperture of $A_N = 0.95$. The determination of the roughness values was performed with MountainsMap 7 (Digital Surf, France). The roughness parameters were determined according to DIN EN ISO 21920–3 with a cut-off wavelength $\lambda_c = 0.25$ mm.

In order to investigate the surface condition in detail specimens were examined additionally with an atomic force microscope (AFM). These measurements were recorded with a Veeco Dimension Icon Scanning Probe Microscope (Veeco Instruments, USA) equipped with a NanoScope V Controller and an AVH-100 workstation. The microscope operated in tapping mode using commercial Tapping Mode Etched Silicon Probes (RTESPA) at various frequencies of $f = 230 \dots 420$ kHz. This enabled a scan speed of 1 \dots 1.3 Hz and a resolution of 512 samples per line for a scan size of 5 μm^2 . Roughness parameters were then determined using the NanoScope 1.5 Software (Bruker Corporation, USA).

2.3.3 Scanning electron microscopy (SEM)

For the high-resolution evaluation of the etched substrates and of the micromilling tools conditioned, the TESCAN Mira 3 (TESCAN ORSAY HOLDING, Czech Republic) scanning electron microscope (SEM) was used. This allowed to complementary evaluate the changes in the cutting edge geometry after preparation. Furthermore, the tools used were assessed regarding the occurrence of signs of wear. In addition to secondary electron (SE) imaging, it was also possible to generate backscattered electron (BSE) images. By using this method, layer defects could be represented in a simplified way.

2.3.4 X-ray analysis

The crystallographic investigations were conducted by a diffractometer Advanced D8 (Bruker AXS, USA) operating in Bragg–Brentano-Setup using a polycap with a diameter of $D = 2$ mm. As source for the x-rays, Co $K\alpha$ radiation was selected with a wavelength of $\lambda = 0.179$ nm and a photon energy of $E = 6.931$ keV. To suppress Co- $K\beta$ radiation, a Fe-filter was selected. For the phase analysis a 2θ range from 20 to 150° with increments of $\Delta 2\theta = 0.035^\circ$ and an

exposure time of $t=0.6$ s were used. The residual stresses in the surface near region were determined by $\sin^2\psi$ method for the WC(112) based on the x-ray elastic constants provided by Eigenmann and Macherauch [34]. The 2θ range was set to 121.5 up to 126.5° with a step size of $\Delta 2\theta=0.1^\circ$ and a measuring time of $t=2$ s. This resulted in a penetration depth of the Co K α radiation of $z_0=1.3$ μm . For the stress analysis, equal distances of $\sin^2\psi$ were selected with values up to 0.5 with rotation angles of $\varphi = \pm 0; 45; 90; 135; 180; 225$ and 270° .

2.3.5 Characterization of the cutting edge geometry

In order to evaluate the influence of the process and the change of the cutting edge condition, the microgeometry of the tools was characterized according to the form-factor method and its parameters of the cutting edge segment on the flank face S_{α} , on the rake face S_{β} and the average cutting edge rounding \bar{S} . All measurements were conducted on a focus variation microscope EdgeMaster (Alicona Imaging, Austria).

2.3.6 Evaluation of coating adhesion

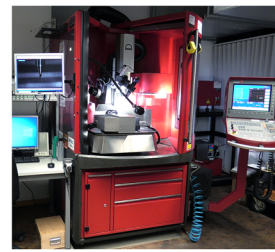
The adhesion of the coating on the differently treated cemented carbide substrates is evaluated by indentation test according to DIN 4856:2018. The classification was conducted ranging from HF1 (excellent adhesion) to HF6 (low adhesion) for the HRA indents (60 kpond). For the statistical evaluation, five indents were performed for each pre-treatment condition.

2.3.7 Evaluation of flank wear land VB

Examinations of the wear condition of tools in use were carried out on a digital microscope VHX-5000 (Keyence, Japan). By using a high magnification lens, high resolution images with up to MAG-1000 \times were generated. This allowed a well-founded evaluation of the signs of wear on the filigree tools. The determination of the width of the flank wear land VB was carried out in the operating software of the measuring system.

2.4 Micromilling

The application tests of the tools were carried out on a micro machine tool HSPC 2522 (Kern Microtechnik, Germany). Due to the high positioning accuracy of ± 0.001 mm and a working accuracy of ± 0.0025 mm, the system is particularly suitable for high-precision micromachining processes. By setting up the 3-axis tool machine in a



KERN HSPC 2522	
Control:	Heidenhain iTNC 530
Spindle:	VSC 4084
max. speed n :	50,000 rpm
Acceleration a :	2,000 mm/s ²
Positioning accuracy:	± 0.001 mm
Repeatability:	± 0.001 mm
Working accuracy:	± 0.0025 mm
Tool holder:	HSK25
Chuck:	shrinking chuck
Cutting fluid application: flood lubrication	

Fig. 2 Machine tool KERN HSPC 2522

Table 2 Process parameters for basic investigation of AEGD-IE

Experiment	Bias voltage U_B	Preparation time t_p
1	– 100 V	60 min
2	– 200 V	60 min
3	– 300 V	60 min
4	– 400 V	60 min
5	– 500 V	60 min
6	– 300 V	30 min
7	– 300 V	90 min
8	– 400 V	120 min
9	– 400 V	240 min
10	– 400 V	360 min
11	– 400 V	480 min
12	– 400 V	600 min

temperature-controlled laboratory on a polymer concrete foundation, the dynamic and thermal disturbances could be limited to a large extend. In addition, the VSC 4084 spindle (Precision, Germany) with a maximum speed of $n=50,000$ rpm enabled the use of finely balanced HSK25 shrink chucks. The machine tool as well as the experimental setup for the deployment tests can be seen in Fig. 2.

The detailed evaluation of cutting forces was performed using a piezoelectric multicomponent dynamometer of type MicroDyn 9109 AA (Kistler Instrumente AG, Switzerland). The measuring device has a high eigenfrequency $f_n(x, y, z) > 15$ kHz, a low response threshold of 0.002 N and is capable of recording small forces at a sampling rate of 150 kHz. After amplification of the force signals by a charge amplifier of type 5080 A (Kistler Instrumente AG, Switzerland) the process forces were filtered with the software NI Diadem 2021 (National Instruments, USA). Filtering was carried out using a Butterworth IIR low-pass filter with a cut-off frequency of $f_c=8$ kHz and a filtering degree of 16. An automated analysis of the force records enabled the evaluation of approximately 5000 tool engagements, which allowed a profound assessment of the operational behavior.

2.5 Design of experiments

The analysis of the material removal by AEGD-IE was performed on the round specimens of ultrafine grain cemented carbide. The bias voltage U_B and the preparation time t_p were varied to evaluate the process behavior. Variation ranges of $U_B = -100 \dots -500$ V and $t_p = 30 \dots 90$ min were selected. Furthermore, the long-term observation was performed with a fixed bias voltage of $U_B = -400$ V up to a preparation time of $t_p = 600$ min. The experimental design for the fundamental process investigation can be seen in Table 2. The prepared substrates were used to evaluate the etch rate as well as the influence of the preparation process on the surface roughness as well as the sub-surface condition.

Furthermore, the interference of the preparation with the PVD coating process was evaluated. For this purpose, samples were modified according to the parameter configurations of experiments 1 ... 5 of Table 2 and subsequently coated with Arc-TiAlN. This analysis mainly focused on the impact on the coating adhesion, which was evaluated in an indentation testing.

The initial investigation on the influence of the AEGD-IE preparation on the microgeometry of the cutting edges was carried out with a fixed bias voltage of $U_B = -400$ V and a varying preparation time of $t_p = 120 \dots 600$ min. The aim was to achieve different amounts of material removal and thus also varying sizes of the cutting edge geometry by varying the process time. The preparation was performed on conventional and uncoated micro end mills with a diameter of $D = 1$ mm, see Sect. 2.1.3.

Based on the investigation of the process impact on microgeometry, a targeted preparation of micro end mills for an operational evaluation was carried out. Due to the given process configuration and the process-specific characteristics of micromachining, reduced preparation parameters were selected in order to assess suitable cutting edge geometries. The preparation was performed with a fixed bias voltage of $U_B = -300$ V and varying process time $t_p = 5 \dots 120$. Following the preparation, the tools were coated with a HiPIMS-TiAlSiN thin film to be suitable for a hard machining process.

The tools were then used for the machining of the hardened high-speed steel AISI M3:2, see Sect. 2.1.2. The machining was performed in a down milling operation in dry conditions, i.e. without additional cooling lubricant. Five

Table 3 Process parameters for the machining of AISI M3:2

Machining parameters	
Depth of cut a_p	25 μm
Width of cut a_e	200 μm
Feed per tooth f_z	25 μm
Cutting speed v_c	120 m/min

measurements of the process forces were carried out over a tool life considered of $l_f = 7.7$ m. The cutting parameters of the machining test can be seen in Table 3. The process forces were determined according to Sect. 2.4. Additional evaluations of the surface roughness achieved were conducted in the initial state of the tools and at the end of the tool life considered.

3 Results and discussion

Following, the fundamental investigations on the AEGD ion etching of specimens of ultra-fine cemented carbide are discussed. The analysis of the etch rate is followed by the evaluation of the impact of AEGD-IE on the surface in general, e.g. the resulting roughness and sub-surface constitution. Furthermore, the influence of intensified preparation on coating adhesion is considered. Based on initial findings, the cutting edge preparation of micro end mills is addressed. Here, the focus is initially on influencing the cutting edge geometry of uncoated tools in order to narrow down the preparation parameters on the basis of the achievable geometry. Subsequently, results are presented for the modification of usable tools where the cutting edge geometry is more specifically adapted to the machining scenario. These tool modifications were carried out with directly subsequent deposition of a PVD coating. Finally, results of first application tests using AEGD-IE modified tools are presented.

3.1 Fundamental analysis of the AEGD-IE process

3.1.1 Determination material removal and etch rate

The material removal in an AEGD ion etching process can be closely linked to the time of preparation t_p as well as the bias voltage U_B applied. This was analyzed on the coin-shaped substrates according to the procedure described in

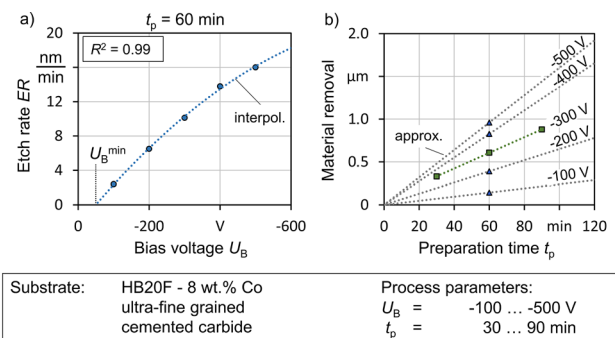


Fig. 3 **a** Etch rate as a function of bias voltage at a preparation time of $t_p = 60$ min and **b** material removal achieved with varying preparation time t_p and bias voltage U_B on specimens

Sect. 2.1 for the given AEGD process configuration. Taking into account the selected preparation time, the etch rate (ER) could be determined over varying bias voltages U_B , see Fig. 3a). Only a small variance of the measured data was observed with $\Delta ER = \pm 0.3$ nm/min for all bias voltages selected Table 3.

As can be seen, a steady non-linear increase of the etch rate was determined with rising bias voltage. This resulted in a maximum etch rate $ER = 15.58 \pm 0.15$ nm/min for $U_B = -500$ V. Furthermore, the data obtained indicate that a minimum bias voltage is necessary to achieve a material removal. This can be attributed to the influence of the bias voltage on the acceleration of the ions toward the substrate surface and thus on the kinetic energy at impact. To achieve an impact cascade at the atoms of the superficial layers, a minimum kinetic energy is required. This depends on the binding energy of the material to be etched. An approximation function of the ER was determined with a 2nd degree polynomial achieving a high coefficient of determination with $R^2 = 0.99$. Based on the approx. function, a minimum bias voltage was calculated to achieve a material removal of $U_{B,min} = -50.8$ V.

$$ER = -3.67 \cdot 10^{-5} \cdot U_B^2 - 5.48 \cdot 10^{-2} \cdot U_B - 2.69 \frac{nm}{min}$$

Furthermore, a linear correlation with respect to the resulting material removal was determined with varying the preparation time t_p at a bias voltage of $U_B = -300$ V, see Fig. 3b). Based on the observation, the prognoses for the material removal of the additional bias voltages were added. Based on the results, the material removal achieved with AEGD-IE on the coin-shaped substrates can thus be predicted precisely and reproducibly. However, it must be taken into account that the material removal achieved also depends on the geometry of the object. For this reason, real milling tools have to be investigated to determine the influence of the geometry and the local etching rates.

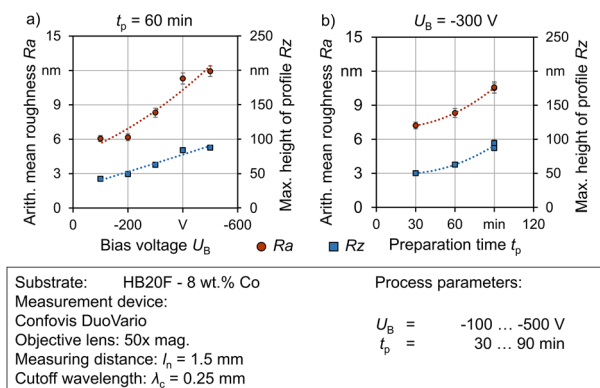


Fig. 4 a Influence of bias stress U_B and b preparation time t_p on the resulting surface roughness of ultrafine grain carbide

3.1.2 Influence of the AEGD-IE on the surface topography

The surfaces were further analyzed after preparation with the confocal microscope DuoVario to evaluate the impact on the resulting surface roughness. The influence of the bias voltage on the roughness parameters of the maximum height of profile Rz and the arithmetic mean roughness Ra is illustrated in Fig. 4a). With rising bias voltage, an increase in the roughness parameters can be observed, starting from the initial, metallurgically prepared condition of the surface. This can be attributed to the stronger removal of the Co matrix as well as the increased exposure of the WC carbides [29, 35]. However, this certain rise in roughness can be considered beneficial for the adhesion of subsequently applied coatings. On the one hand, the layer growth predominately takes place on the WC carbides and thus on the hard material phase. On the other hand, this leads to better mechanical bonding of the coating to the surface of the substrate [36]. Furthermore, an increase in deviations was recorded at a bias voltage of $U_B = -500$ V, which can be attributed to the stronger alteration of surface topography. A detailed discussion of the effect is conducted in subsequent sections.

Furthermore, comparable to the influence of the bias voltage, an increase in roughness along the preparation time was observed, as presented in Fig. 4b). This effect can be attributed to the prolonged duration of the ion bombardment and consequently an increased influence of the AEGD-IE preparation. Moreover, the impact of the preparation was analyzed for longer treatments with $U_B = -400$ V. Here, a maximum preparation time of $t_p = 600$ min was considered, see Fig. 5.

Based on the values obtained, an almost linear increase of the arithmetic mean roughness can be stated for preparation times up to 360 min, which changes into an asymptotic behavior for longer preparation times and a bias voltage of $U_B = -400$ V. For the given process setup, this results in roughness values of $Rz = 135 \pm 9$ nm and $Ra = 15.3 \pm 0.4$ nm. The reason for this behavior can be attributed to the constitution of the cemented carbide substrate. For lower levels of bias voltage, respectively a lower energy of the Ar⁺ ions, a predominantly etching of the Co binder phase can

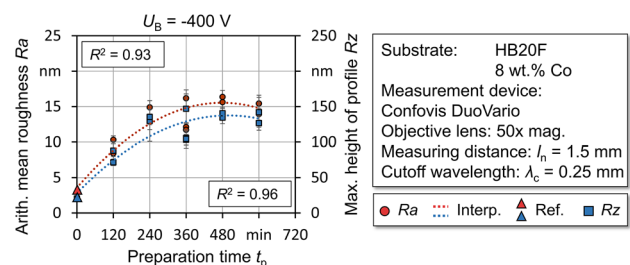


Fig. 5 Influence of the preparation time t_p on the surface roughness

be concluded, which was also observed by Gassner et al. for cutting inserts [29]. After the removal of the Co matrix, the WC grains are exposed on the surface and are etched as well over the duration of the treatment. However, this leads to small changes in the geometry of the grains, which do not show a change of the roughness profile with longer exposure time. In particular, the specification of the substrate respectively the cemented carbide has a significant influence in this respect since different topographies can be expected based on the WC grain size and the binder content. Due to the consideration of a cemented carbide of type HB20UF with a grain size of $d_k = 0.2 \dots 0.5 \mu\text{m}$, the low maximum roughness values can be concluded.

For a better understanding of the involved mechanisms analyses of the surface topography, the etched substrates were examined using an AFM microscope. Figure 6 depicts the surface topographies, which were exposed to the different levels of bias voltage. As presented by the initial polished surface, a smooth surface with no differentiation between hard phase and matrix is observed. It can be assumed that the Co binder phase was predominantly located on the surface due to the metallurgical preparation of the specimens. However, already with a low bias voltage of $U_B = -100 \text{ V}$, an erosion of the Co matrix can be detected. Consequently, the WC carbides are exposed underneath, resulting in a rougher surface topography. This effect is intensified with increasing bias voltage. Above $U_B = -300 \text{ V}$, however, an increasing influence of the carbides can be observed. In particular, the maximum voltage considered achieved a roughened surface.

In order to quantitatively evaluate the alterations, areal roughness parameters were determined. As can be seen from Fig. 7, an increase in roughness comparable to the roughness analysis with the confocal surface measuring instrument can be observed. The alteration of the surface characteristics is also evident in the areal parameter of the skewness Ssk seen in Fig. 7c) as well as the material ratios visible in Fig. 7d), which were determined based

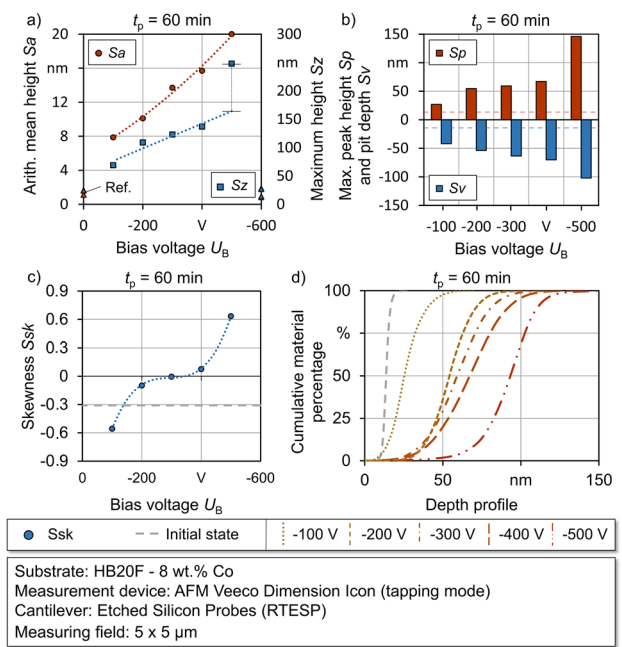


Fig. 7 Characterizations of the areal roughness: **a** arith. mean height Sa and maximum height Sz ; **b** maximum peak height Sp and pit depth Sv ; **c** skewness Ssk ; **d** the cumulative material ratio

on the AFM measurements. The increasing exposure of the carbides initially results in a topography of greater depth and a more symmetrical height distribution for a bias voltage of $-100 \text{ V} < U_B < -400 \text{ V}$. Noticeable, however, is the disproportionate increase of the maximum height Sz at a bias voltage of $U_B = -500 \text{ V}$ (Fig. 7a)). The increase in surface defects as well as the change in the characteristics of the topography are also evident in the areal parameter values of the maximum height Sz , the maximum peak height Sp and the skewness Ssk , which show a disproportionate increase in roughness, see Fig. 7. The surface defects were attributed to the occurrence of local arc discharges on the substrate holder system due to the applied high electrical potential.

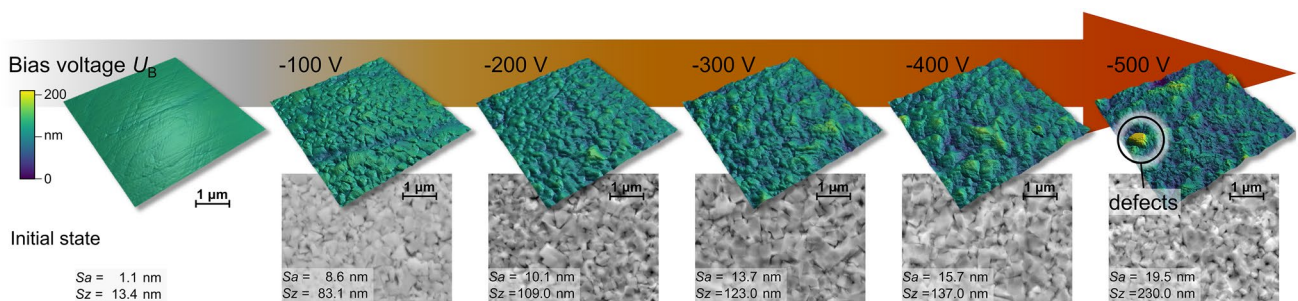


Fig. 6 Effect of increasing bias voltage on the topography of ultrafine grain carbide shown on SEM and AFM micrographs

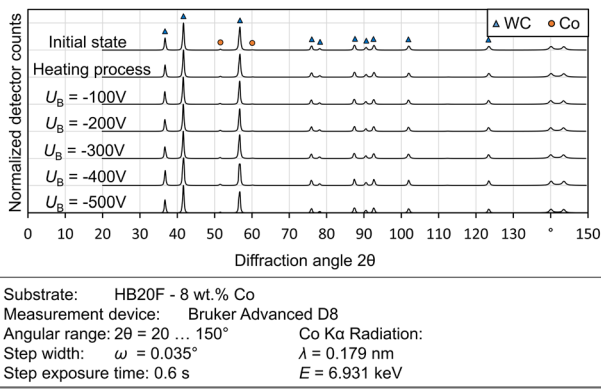


Fig. 8 Phase analysis of substrate sub-surface after AEGD-IE of coin-shaped specimens with varying bias voltage U_B

3.1.3 Influence of the AEGD-IE on the sub-surface constitution

The high-energy ion etching process demands an evaluation of possible changes in the phase composition of substrate in order to sufficiently set the process parameters for a targeted preparation. For this purpose, a phase analysis was performed on the coin-shaped substrates of ultrafine grain cemented carbide and varying bias voltages. The analysis was based on x-ray diffraction according to the procedure described in Sect. 2.3.4. The results of the phase analysis with respect to varying bias voltages can be seen in Fig. 8.

Based on the analyses, almost identical results of the phase composition were determined starting from the initial state over the heating and etching process. As can be seen in Fig. 8, all samples exhibit the reflections of the WC phase to the same comparable extent. Based on these results, no significant changes in the WC phases, e.g., degradation process to W_2C , were detected. In particular, at the highest bias voltage considered of $U_B = -500 \text{ V}$, no negative influences of the AEGD-IW preparation process on the substrate

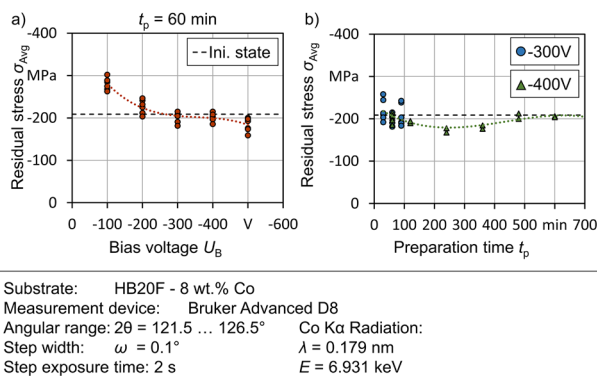


Fig. 9 **a** Residual stress state in dependence of the bias voltage U_B and **b** the preparation time t_p in AEGD-IE of coin-shaped specimens

sub-surface could be determined. Thus, no process limits with respect to the choice of bias voltage were identified in the course of the investigations.

Furthermore, the resulting residual stress state of the substrates was observed after preparation. As can be seen from Fig. 9a), a minor dependence of the resulting compressive residual stresses on the variation of the bias voltage was observed at a penetration depth of radiation of $z_0 = 1.3 \mu\text{m}$. Low bias voltages of $U_B \geq -200 \text{ V}$ resulted in a small decrease in compressive residual stresses compared to the initial condition, which can be explained by the increased thermal energy level, which results from the higher kinetic energy during the etching process. This leads to a thermally induced relaxation of the compressive residual stress and thus a shift towards lower compressive stresses. Disregarding such effects, a process window of $U_B = -200 \dots -400 \text{ V}$ was determined in which no significant alteration occurs.

Furthermore, the change in residual stresses over the preparation time was considered for the bias voltages of $U_B = -300 \text{ V}$ and -400 V , see Fig. 9b). No significant changes were observed up to a preparation time of $t_p = 10 \text{ h}$. This provides unrestricted flexibility for the process design with regard to the preparation time. Consequently, the preparation can be extended as required for the adjustment of a cutting edge geometry. The investigation of the bias voltage resulted in a relevant process window, which ensures a high material removal without affecting the phase composition and only slightly the residual stresses in the substrate material.

3.1.4 Coating adhesion of an Arc-TiAlN coating

Based on the previous investigations, a positive influence of the surface and sub-surface condition for a subsequent coating process can be assumed. The coating adhesion was further investigated on the coin-shaped substrates with varying preparation time t_p and bias voltages U_B . Following the

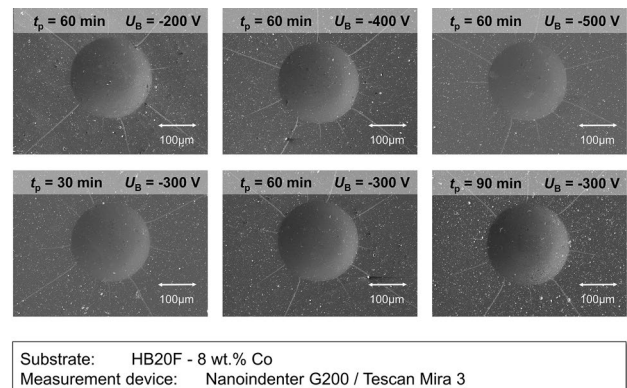


Fig. 10 Coating adhesion test results of Arc-TiAlN after Rockwell indentation of modified HB20UF specimens

preparation by AEGD-IE, an Arc-TiAlN coating was deposited on all samples and the resulting coating adhesion was evaluated by means of Rockwell indentation test according to DIN EN ISO 26443. The analysis showed an overall high adhesion of the coatings for all specimens. An adhesion of class HF1 was determined for all coated specimens, see Fig. 10.

As can be seen, all parameter combinations led to a high degree of the coating adhesion and no adverse effects for coating deposition were determined. It can therefore be stated that, due to the actual function of ion etching process, no detrimental influences result even with intensified conditioning parameters of the surface. This allows flexible adaptation of the cleaning process to change not only the conditioning of the substrates surface but also the properties of the cutting edge.

3.2 Cutting edge preparation of micro end mills

Based on the fundamental analysis, it could be shown that the intensified AEGD-IE process results in an advantageous condition of the surface and sub-surface achieving a high layer adhesion. Consequently, it has to be examined whether

suitable cutting edge geometry can be achieved by adapting the AEGD-IE process. Thus, based on the recorded fundamentals of material removal, modifications of micro end mills with a diameter of $D = 1$ mm were conducted. In order to achieve a high material removal rates and to investigate the possible magnitude on the cutting edge geometries to be obtained, the conditioning was initially carried out with a fixed bias voltage of $U_B = -400$ V and a varying preparation time of $t_p = 120 \dots 600$ min. The deposition of a PVD coating was initially omitted for analytical purposes.

Figure. 11 shows several cutting edge profiles of different tools, which show an increase in size depending on the preparation time. The preparation of the tools resulted in an asymmetric and chamfer-like cutting edge geometry, with a steady runout to the rake face Fig. 10. On the side of the flank face, on the other hand, a more sharp transition of the microgeometry was produced. From the initial geometry, an intensified influence on the cutting edge segment of the rake face S_γ can be determined for the given process configuration as well as substrate holder system used. Noticeable is also an alteration of the wedge angle β of the tools, which will be addressed later on. Fig. 12 shows scanning electron micrographs of the modified tools with detailed views of the cutting corner and the minor cutting edge. The impact of the preparation on the magnitude of the cutting edge geometry becomes evident. With increasing preparation time, a stronger change in geometry can be observed. The increased material removal at the cutting edges can be attributed to the increased density of electric field lines. Therefore, comparable to abrasive blasting processes, the edges are etched intensively. For quantitative analysis, all cutting edges were measured with a focus variation microscope, see Sect. 2.3.5. The characteristic values determined of the average cuttings edge rounding \bar{S} and the form-factor K can be seen in Fig. 13. An almost linear increase in the average cutting edge rounding was determined with increasing preparation time, see Fig. 13a). After a maximum preparation

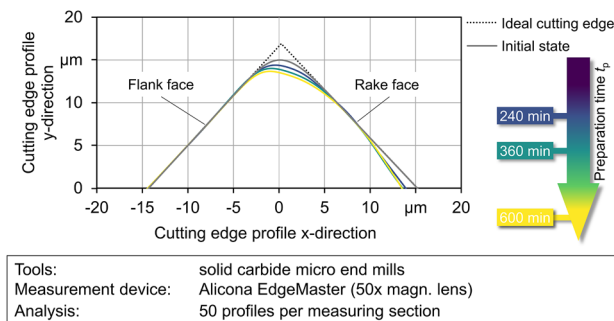


Fig. 11 Profiles of microgeometries after varying preparation time t_p

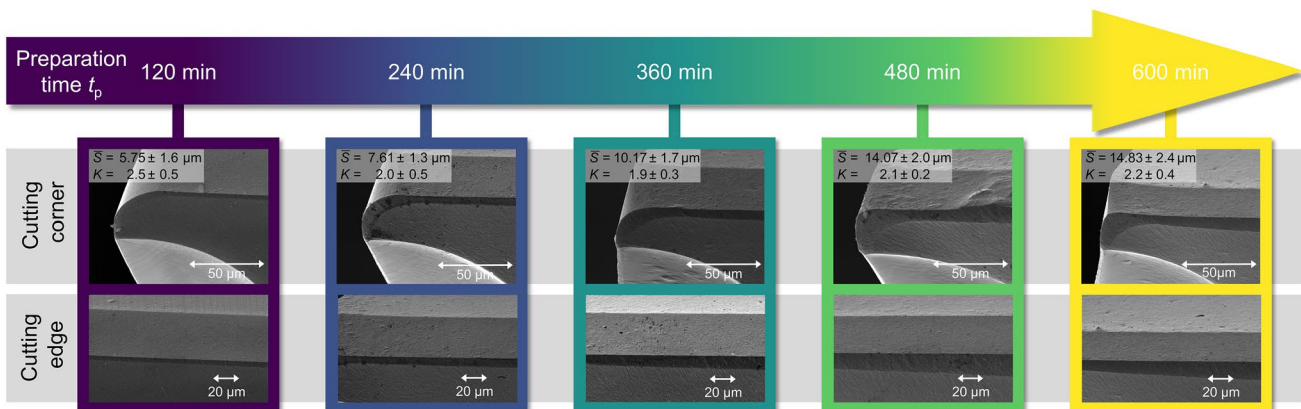


Fig. 12 Scanning electron micrographs of micro end mills modified using AEGD-IE and varying preparation time

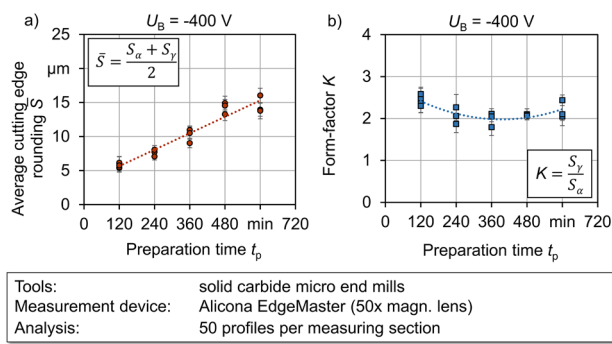


Fig. 13 Characterization of the cutting edge geometry modified using AEGD-IE and varying preparation time

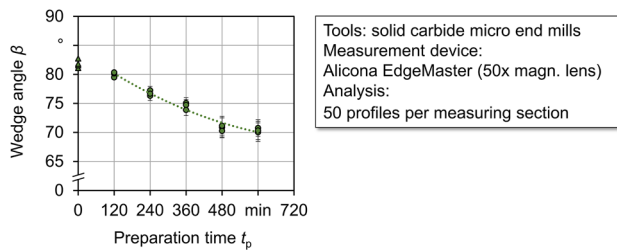


Fig. 14 Variation of the wedge angle β along the preparation time t_p

time of $t_p = 600$ min, an average cutting edge rounding of $\bar{S} = 14.83 \pm 2.4 \mu\text{m}$ was determined. As can be seen Fig. 13b) complementary to Fig. 11, asymmetric cutting edge geometries with a form-factor of $K > 1$ were obtained. Specifically, values of $1.9 < K < 2.5$ were achieved. After evaluating the microgeometry, it becomes evident that all cutting edges predominantly exhibited a comparable level of the form-factor with a low variance of the measured data. It was therefore possible to reproducibly achieve oriented cutting edge geometries with varying sizes in the preparation setup. Considering the established basic knowledge of cutting edge preparation, the form factor achieved can be rated as advantageous due to the increased preparation of the rake face [2]. It has to be mentioned that the form-factors were relatively high, considering the expected optimum values in literature. However, this highlights the potential of the process approach of AEGD-IE for cutting edge preparation. In particular, the smaller cutting edge geometries represent a relevant possibility for optimizing filigree precision tools due to the nevertheless clearly pronounced asymmetry of the cutting edge.

Further evaluation of the preparation result showed an impact on the cutting edge corner as well as on the surface topography as the ion bombardment affects the entire tool geometry. Especially with a long preparation time of

$t_p > 360$ min, a macroscopic change in the shape of the tools were evident, see Fig. 12. The increased material removal of the AEGD-IE process thus leads to a change in the overall tool geometry, which is particularly noticeable from the degradation of the corner radius as well as the wedge angle. The latter were considered based on the determined angles of the cutting wedge. As can be seen in Fig. 14, a decrease in the wedge angle β was observed with increasing preparation time. Starting from the initial wedge angle of $\beta = 80^\circ$, a reduction to $\beta = 70^\circ$ was recorded after $t_p = 600$ min. This significant change in the overall shape of the tool demonstrates the high material removal rates in an AEGD-IE process. Consequently, when modifying tools more intensively, the impairment of the macroscopic tool shape must also be taken into account.

As the results show, AEGD-IE can be adapted to modify the geometry of cutting edges. It thus represents a relevant new approach for the preparation of cutting edges prior to the coating deposition. In addition to the basic approach, the asymmetric shape achieved in particular represents great potential to produce oriented microgeometries of small scale. By sufficiently designing the process, tools with the smallest diameters can thus be modified without the limitations of mechanical preparation methods. It offers opportunities to overcome previous constraints that hinder the transfer of established knowledge of the favorable cutting edge designs to micromachining.

3.3 Experimental analysis of machining experiments

Based on the process fundamentals shown, tools were modified for initial machining tests. The modification of the tools was carried out with reduced preparation parameters, with respect to the engagement situation of the considered machining process. The aim was to evaluate a process-oriented cutting edge geometry in a micromilling process of AISI M3:2. The preparation was performed with a bias voltage of $U_B = -300$ and varying preparation times of $t_p = 5 \dots 120$ min. Furthermore, tools were conditioned using an energetically weaker ion etching by glow discharge (GD-IE), which served as a reference for this investigation. Due to the lower ionization and material removal rate in this IE-process, an influence on the cutting edge geometry could be limited to a minimal extent. These tools were etched with $t_p = 60$ min and $U_B = -750$ V. The preparation of the cutting edges was followed by the deposition of a HiPIMS-TiAlSiN coating. The coating system was explicitly selected because of its high suitability for hard micromachining of AISI M3:2. The coating was deposited in a HiPIMS process according to Sect. 2.2

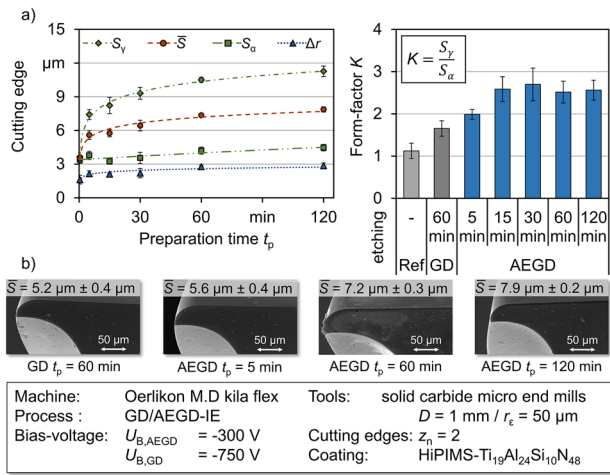


Fig. 15 a Characterization of modified and coated micro end mills and b SEM images of the cutting corners

3.3.1 Characterization of modified and coated end mills

The tools featured a chamfer-like cutting edge geometry after preparation and coating comparable to the previous illustration. Average cutting edge rounding of $\bar{S} = 5.20 \dots 8.25 \mu\text{m}$ were determined using a focus variation microscope, see Fig. 15a). With regard to the orientation of the cutting edge, a form-factor of $K \sim 2.5$ was determined for most tools. However, this differed on tool, which were only prepared for a short process time of $t_p = 5$ min. This was attributed to the low material removal and thus smaller change in geometry. Furthermore, an increase in the size of the cutting edges rounding \bar{S} was observed due to coating application, which can be attributed to the layer thickness deposited. Because of a reduced, maximum preparation time of $t_p = 120$ min, macroscopic changes in the geometry of the tools were not evident, see Fig. 15b).

3.3.2 Evaluation of process behavior and wear development of modified tools

Following the preparation and characterization, the tools have been used in a micromilling process of the hardened powder metallurgical high-speed steel AISI M3:2. The machining tests were performed according to the procedure illustrated in section 2.5. The progression of the active force F_a , the passive force F_p , and the overall resultant force F_z recorded can be seen in Fig. 16.

At the beginning of the tool life, all tools showed a comparable level of machining forces. Depending on the average cutting edge rounding, a minor increase of the resultant forces was determined with larger roundings.

A more deviating process behavior was observed after a milling path of $l_f = 2$ m for the tools with the shortest

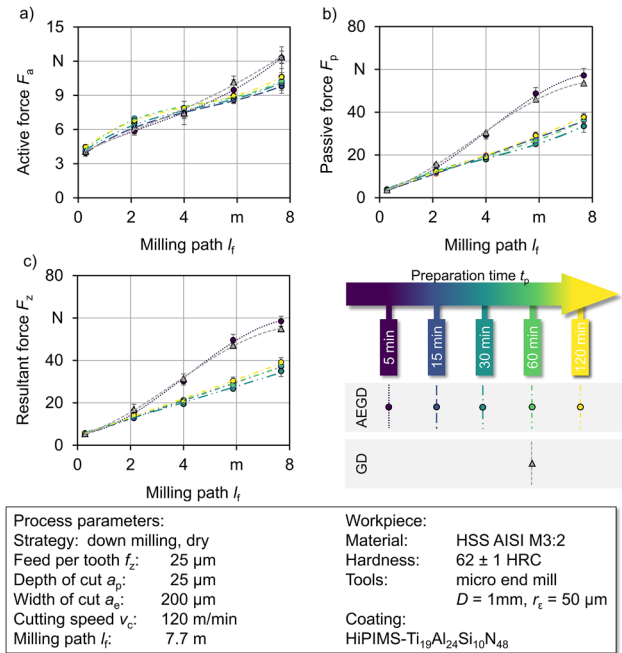


Fig. 16 Progression of the machining forces: a active force F_a ; b passive force F_p and c the resultant force F_z over the service life

preparation time ($t_p = 5$ min) as well as the tools prepared by GD-IE. This is particularly evident in the rise of the passive forces indicating a stronger wear development of the tools, see Fig. 16b).

In the following, the process forces are discussed at the end of the tool life travel path considered, taking into account the determined average cutting edge rounding \bar{S} of the cutting edges, see Fig. 15. Whereas initially only a minor dependency of the cutting edge geometry on the process forces could be seen, more divergent process behaviors were evident at the end of the tool life. As can be seen from Fig. 17 a), the tools with an average cutting edge rounding

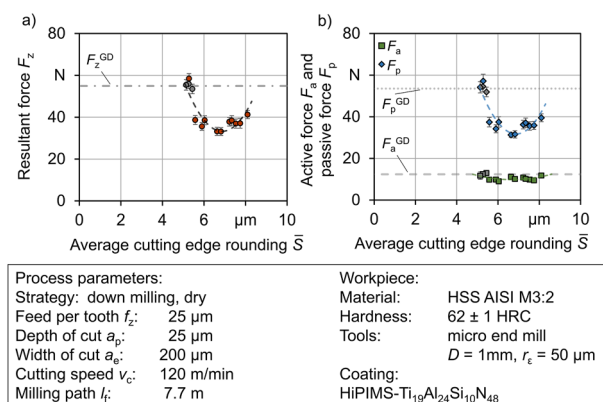


Fig. 17 a Resultant force F_z ; b active force F_a and passive force F_p in dependence of the average cutting edge rounding \bar{S}

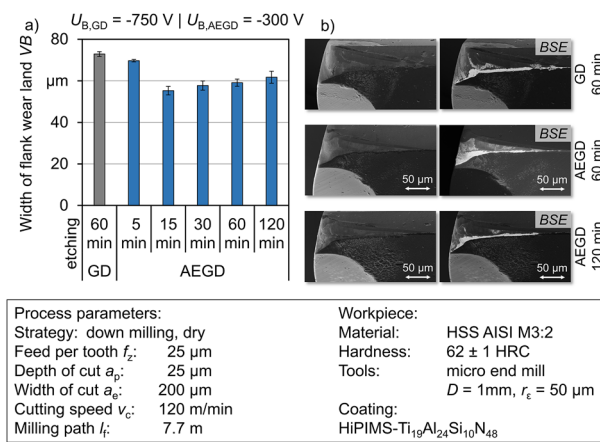


Fig. 18 a Wear analysis of modified and used tools based on the width of the flank wear land VB ; b SEM images of the cutting edge corner

of approx. $\bar{S} = 6.5 \mu\text{m}$ achieved the lowest resultant force in the investigation. This corresponds to a preparation time of $t_p = 30$ min. Predominantly, the process forces are attributable to the decisive share of passive forces, see Fig. 17b). This indicates a reduced wear development and consequently minor alteration of the cutting edge geometry due to the preparation setup. A larger or smaller cutting edge rounding, however, led to higher resultant forces respectively passive forces.

Following the analysis of the resulting process forces, the wear development of the tools was evaluated by means of the width of flank wear land VB and scanning electron micrographs. As can be seen from Fig. 18a), the tools with $t_p = 5$ min in particular exhibited the largest wear lands of the tools modified by AEGD-IE. This corresponds to the observations of the strongest rise in the resultant force, see Fig. 15a). Based on the SEM images, on the other hand, no obvious layer delamination was detected, which would indicate reduced layer adhesion due to the short preparation time. In general, however, it must be taken into account that due to the interaction effects of the surface pretreatment and the cutting edge preparation, a minimum preparation time must be maintained in order to ensure a sufficient coating adhesion. Furthermore, the lowest level of wear on the tools was achieved with a preparation time of $t_p = 15$ min. Proceeding from this, a resumed increase of the width of the flank wear land was detected with increasing preparation time, respectively the average cutting edge rounding. As a result, the tools that exhibited the lowest resultant force ($t_p = 30$ min) also showed a slightly stronger wear development. In particular, tools with longer preparation times consequently showed increased signs of wear. Referring to the initial process forces, it can be expected that due to

the stronger preparation of the edge shape as well as the resulting process forces, a larger mechanical load acts on the tools. Excessive preparation of the edge shape thus leads in turn to a deterioration of the enhanced process behavior Fig. 18.

Based on the results shown, it can be stated that with the given design of the cutting process and based on the varied preparation parameters, an advantageous cutting edge shape could already be achieved with a preparation time of $t_p = 15 \dots 30$ min. This initially demonstrates that a modification of the cutting edge shape can be carried out on precision tools for micromachining within a short process time. The technological approach thus represents great potential for scientific and industrial applications.

4 Summary and outlook

A new approach for cutting edge preparation of precision tools by ion etching in the PVD process was presented. In this context, fundamental investigations on the influence of AEGD-IE on the surface topography and sub-surface condition were presented. In addition, the resulting coating adhesion of an Arc evaporated TiAlN coating was analyzed on substrates of ultrafine grain cemented carbide. Based on the etch rates determined, the conditioning of conventional uncoated micro end mills was investigated with extended preparation time. As shown, chamfer-like and asymmetric cutting edge geometries of different sizes could be produced in the considered experimental setup. Based on the identified potentials of the approach, milling tools were further conditioned and subsequently coated with a HiPIMS-TiAlSiN coating in a single process run. The application tests indicated high potentials regarding the process forces and wear behavior at short preparation times of $t_p = 15 \dots 30$ min. Considering the required conditioning of the substrate surface that has to be performed for high coating adhesion, this represents an efficient approach of a simultaneous preparation of the cutting edge. The most important findings can be summarized:

- For the etch rate of varying bias voltages as well as different preparation times, correlations could be derived with high accuracy for the ultrafine grain cemented carbide considered.
- The topographical change in the AEGD-IE process could be shown based on the parameter variation. This analysis indicated a favorable process window of the bias voltage of $U_B = -200 \dots -400$ V.
- Process times of the etching process ($t_p > 360$ min) showed an asymptotic development of the roughness profile.

- Based on the analysis of the sub-surface of the substrate for all levels of bias voltage compressive residual stresses could be determined.
- The evaluation of the coating adhesion on the differently treated substrates showed an adhesion class HF1 for all conditions. Accordingly, no impairment results even with more intensive conditioning.
- The preparation of micromilling tools resulted in an oriented, chamfer-like cutting edge geometry with a form-factor $K = 2.0 \dots 2.4$. By varying the preparation time t_p , different average cutting edge roundings \bar{S} could be achieved.
- Machining tests of the modified and coated tools revealed a reduction of process forces and beneficial process behavior for an average edge rounding of $\bar{S} = 5.5 \dots 6.5 \mu\text{m}$. With the given configuration of the preparation process, these tools were modified within $t_p = 15 \dots 30 \text{ min}$.

Based on the results, a strong potential of the approach could be demonstrated. At the present time, however, the fully comprehensive adjustment of the cutting edge geometry has not yet been achieved. Further research is necessary in order to be able to specifically influence the orientation of the cutting edge geometry, respectively the form-factor. By identifying further process parameters, a flexible design of the microgeometry can be achieved.

In addition, economic aspects as well as the integration into an existing process chain for the manufacturing of tools should be investigated in detail. Compared to established processes for cutting edge preparation, e.g. abrasive blasting or drag finishing, the utilization of AEGD ion etching to prepare the cutting edge holds the potential to reduce the overall process duration in tool manufacturing. Despite the comparatively extended etching times, it is noteworthy that the PVD chamber can accommodate a large number of tools. This capability allows for the cutting edge preparation of multiple tools, ensuring a cost-effective and time-efficient process. Furthermore, the use of additional AEGD modules to increase the etching rate and, consequently, to reduce the process time for the cutting edge preparation is presently unclear and necessitates further investigation.

Acknowledgements This research was funded by the Deutsche Forschungs-gemeinschaft (DFG, German Research Foundation)—Effects and interactions for interface and cutting-edge conditioning in hard micromachining—project number 445127534 and Process and tool development for micromilling of cemented carbides – project number 504088406. Furthermore, the authors would like to thank Mr. Volker Brandt of the Chair of Biomaterials and Polymer Sciences (TU Dortmund University) for providing and supporting the AFM measurements.

Funding Open Access funding enabled and organized by Projekt DEAL.

Declarations

Conflict of interest The authors declare that they have no conflict of interest.

Open Access This article is licensed under a Creative Commons Attribution 4.0 International License, which permits use, sharing, adaptation, distribution and reproduction in any medium or format, as long as you give appropriate credit to the original author(s) and the source, provide a link to the Creative Commons licence, and indicate if changes were made. The images or other third party material in this article are included in the article's Creative Commons licence, unless indicated otherwise in a credit line to the material. If material is not included in the article's Creative Commons licence and your intended use is not permitted by statutory regulation or exceeds the permitted use, you will need to obtain permission directly from the copyright holder. To view a copy of this licence, visit <http://creativecommons.org/licenses/by/4.0/>.

References

1. Bassett E, Köhler J, Denkena B (2012) On the honed cutting edge and its side effects during orthogonal turning operations of AISI1045 with coated WC-Co inserts. *CIRP J Manuf Sci Technol* 5(2):108–126
2. Denkena B, Biermann D (2014) Cutting edge geometries. *CIRP Ann* 63(2):631–653
3. Bouzakis K-D, Michailidis N, Skordaris G, Bouzakis E, Biermann D, M'Saoubi R (2012) Cutting with coated tools: Coating technologies, characterization methods and performance optimization. *CIRP Ann* 61(2):703–723
4. Tönshoff HK, Denkena B (2013) Basics of cutting and abrasive processes. Springer, Berlin, Heidelberg, p 399
5. Cortés Rodríguez CJ (2009) Cutting edge preparation of precision cutting tools by applying micro-abrasive jet machining and brushing. Zugl.: Kassel, Univ., Diss., 2009. Kassel Univ. Press, Kassel, p 189
6. Keith J, 1992. Fundamentals of insert edge preparation. *Manufacturing '92-Cutting Tool Geometries*, Sep. 1992, Chicago
7. Denkena B, Reichstein M, Brodehl J, León García de L 2005. Surface preparation, coating and wear performance of geometrically defined cutting edges. *Proceedings of the 5th international conference the coatings in manufacturing engineering*, 5–7
8. Denkena B, Koehler J, Rehe M (2012) Influence of the honed cutting edge on tool wear and surface integrity in slot milling of 42CrMo4 steel. *Proced CIRP* 1:190–195
9. Wyen C-F, Wegener K (2010) Influence of cutting edge radius on cutting forces in machining titanium. *CIRP Ann* 59(1):93–96
10. Yen Y-C, Jain A, Altan T (2004) A finite element analysis of orthogonal machining using different tool edge geometries. *J Mater Process Technol* 146(1):72–81
11. Bouzakis K-D, Skordaris G, Gerardis S, Katirtzoglou G, Makri-mallakis S, Pappa M, Bolz S, Koelker W (2010) The effect of substrate pretreatments and HPPMS-deposited adhesive inter-layers' materials on the cutting performance of coated cemented carbide inserts. *CIRP Ann* 59(1):73–76
12. Denkena B, Lucas A, Bassett E (2011) Effects of the cutting edge microgeometry on tool wear and its thermo-mechanical load. *CIRP Ann* 60(1):73–76
13. Fang N, Wu Q (2005) The effects of chamfered and honed tool edge geometry in machining of three aluminum alloys. *Int J Mach Tools Manuf* 45(10):1178–1187
14. Shaw MC, Shaw MC (2005) *Metal cutting principles*, 2nd edn. Oxford University Press, New York, p 651

15. Bassett E (2014) Belastungsspezifische Auslegung und Herstellung von Schneidkanten für Drehwerkzeuge. Zugl.: Hannover, Univ., Diss., 2013. PZH-Verl, Garbsen, p 188
16. Rech J 2005. Cutting Edge Preparation and Surface Issues. HSS Forum's Int. Con. "Smart solutions for metal cutting", 1–12
17. Wyen C-F 2011. Rounded cutting edges and their influence in machining titanium
18. Meijer AL, Stangier D, Tillmann W, Biermann D (2022) Induction of residual compressive stresses in the sub-surface by the adjustment of the micromilling process and the tool's cutting edge. *CIRP Ann* 71(1):97–100
19. Tillmann W, Stangier D, Meijer A, Krebs E, Ott A, Platt T, Lopes Dias NF, Hagen L, Biermann D (2022) Adapting the surface integrity of high-speed steel tools for sheet-bulk metal forming. *JMMP* 6(2):37
20. Wild T, Platt T, Biermann D, Merklein M (2021) Analysis of the influence of surface modifications on the fatigue behavior of hot work tool steel components. *Materials* 14(23):324
21. Baharudin BHT, Dimou N, Hon KKB (2004) Tool wear behaviour of micro-tools in high speed CNC machining. In: Hinduja S (ed) Proceedings of the 34th International MATADOR Conference. Springer, London, London, pp 111–118
22. Uhlmann E, Oberschmidt D, Kuche Y, Löwenstein A (2014) Cutting edge preparation of micro milling tools. *Proced CIRP* 14:349–354
23. Uhlmann E, Oberschmidt D, Kuche Y, Löwenstein A, Winker I (2016) Effects of different cutting edge preparation methods on micro milling performance. *Proced CIRP* 46:352–355
24. Krebs E, Wolf M, Biermann D, Tillmann W, Stangier D (2018) High-quality cutting edge preparation of micromilling tools using wet abrasive jet machining process. *Prod Eng Res Devel* 12(1):45–51
25. Bunshah RF (ed) (2001) Handbook of hard coatings: Deposition technologies, properties and applications. Noyes Publ, Park Ridge, NJ, p 550
26. Taglauer E (1990) Surface cleaning using sputtering. *Appl Phys A* 51(3):238–251
27. Anders A (2010) A structure zone diagram including plasma-based deposition and ion etching. *Thin Solid Films* 518(15):4087–4090
28. Lattemann M, Ehiasarian AP, Bohlmark J, Persson P, Helmersson U (2006) Investigation of high power impulse magnetron sputtering pretreated interfaces for adhesion enhancement of hard coatings on steel. *Surf Coat Technol* 200(22–23):6495–6499
29. Gassner M, Schalk N, Sartory B, Pohler M, Czettel C, Mitterer C (2017) Influence of Ar ion etching on the surface topography of cemented carbide cutting inserts. *Int J Refract Metal Hard Mater* 69:234–239
30. Bunshah RF, Blocher JM, Bonifield TD, Fish JG, Jacobson BE, Mattox DM (1982) Deposition technologies for films and coatings: Developments and applications. Noyes Publ, Park Ridge, NJ, p 585
31. Schönjahn C, Bamford M, Donohue LA, Lewis DB, Forder S, Münz W-D (2000) The interface between TiAlN hard coatings and steel substrates generated by high energetic Cr+ bombardment. *Surf Coat Technol* 125(1–3):66–70
32. Vetter J, Wallendorf T (1995) Plasma diagnostics of arc-enhanced glow discharge. *Surf Coat Technol* 76–77:322–327
33. Vetter J, Burgmer W, Perry AJ (1993) Arc-enhanced glow discharge in vacuum arc machines. *Surf Coat Technol* 59(1–3):152–155
34. Eigenmann B, Macherauch E (1996) Röntgenographische Untersuchung von Spannungszuständen in Werkstoffen Teil III Fortsetzung von Matwiss und Werkstofftechn Heft 3/1995, S. 148–160 und Heft 4/1995, S. 199–216. *Materialwissenschaft Werkst.* 27(9):426–437
35. Panjan P, Drnovšek A, Mahne N, Čekada M, Panjan M (2021) Surface topography of PVD hard coatings. *Coatings* 11(11):1387
36. Alves SM, Albano W, de Oliveira AJ (2017) Improvement of coating adhesion on cemented carbide tools by plasma etching. *J Braz Soc Mech Sci Eng* 39(3):845–856

Publisher's Note Springer Nature remains neutral with regard to jurisdictional claims in published maps and institutional affiliations.